International Journal of Biological Macromolecules 181 (2021) 672–682

Contents lists available at ScienceDirect

International Journal of Biological Macromolecules

journal homepage: http://www.elsevier.com/locate/ijbiomac

Characterization of a polysaccharide from the medicinal lichen, *Usnea longissima*, and its immunostimulating effect in vivo

Teng Wang, Chen Shen, Feng Guo, Yuqin Zhao, Jie Wang, Kunlai Sun, Bin Wang, Yan Chen *, Yin Chen *

College of Food and Pharmacy, Zhejiang Ocean University, Zhoushan, Zhejiang 316000, China

ARTICLE INFO

Article history:
Received 7 December 2020
Received in revised form 26 March 2021
Accepted 26 March 2021
Available online 30 March 2021

Keywords:
Polysaccharides
Lichen
Immune system balance
Immunomodulation
Antioxidant
Usnea longissima

ABSTRACT

A polysaccharide, CSL-0.1, was isolated from the medicinal lichen, *Usnea longissima*. CSL-0.1 was a neutral rhamnose-containing glucogalactomannan with a molecular weight of 7.86×10^4 Da. The polysaccharide had a core mannan structure with (1 → 6)-α-D-Man*p* units as the main chain and was substituted at the *O*-2 positions with side chains containing (1 → 2)-α-D-Man*p* residue, [3)-α-Glc*p*(1 → 4)-α-Glc*p*(1→] and 6-*O*-substituted β-D-Gal*f* units. 2-*O*- and 2,3-di-*O*-substituted Rha*p* units. The effects of CSL-0.1 on intestinal immunity and antioxidant activity were evaluated. CSL-0.1 increased the spleen and thymus indices in a dose-dependent manner and conferred immunomodulation on reversing the Th1/Th2-related cytokine imbalance in cyclophosphamide (CP)-induced immunosuppressed mice. CSL-0.1 could also enhance the levels of secretory immunoglobulin A in CP-injected mice. Additionally, the antioxidant levels in the liver and intestine of the mice were increased 20%–50% after intragastric injection by CSL-0.1.

1. Introduction

Usnea longissima is a filamentous lichen found in foggy regions, which especially adheres to pine trees. It is mainly distributed in the northeast, Shaanxi, Zhejiang, and other provinces of China. As a traditional Chinese medicine, *U. longissima* has been used as an expectorant for thousands of years [1] and has also been widely used for pain relief, fever control, and the treatment of ulcers owing to its heat-clearing and detoxifying properties [2]. Moreover, *U. longissima* is the preferred food for the snub-nosed monkey in winter because of its nutritional properties, which helps regulate their intestinal flora and provides energy to sustain the winters [3]. Previous studies have indicated that the extracts or prescriptions of *U. longissima* have several biological activities, including antiplatelet [4], antithrombotic, anti-inflammatory, analgesic, antipyretic, anti-tumor, anti-cholesterol, and nematocidal effects [5].

It has been found that polysaccharides, especially their glycosylated derivates, are crucial in modulating the biological response in the immune system. In addition, most naturally occurring polysaccharides have some level of immunostimulating activity [6]. Apart from the medicinal properties and the high nutritional value of *U. longissima*, it has been reported that the polysaccharides extracted from *U. longissima* are one of the main bioactive ingredients that can scavenge oxygen free radicals, prevent lipid peroxidation, and enhance immunological function [7]. However, to date, limited information is available on the structural characteristics of the polysaccharides from *U. longissima*, as well as its immunostimulating and antioxidant effects in immunosuppressed mice. To better understand and evaluate its therapeutic effects, we aimed to characterize the structure of *U. longissima* and determine its immunostimulating effects.

2. Materials and methods

2.1. Materials and reagents

U. longissima was obtained from Qinling Mountain, Shaanxi Province, China. Female ICR mice (aged 6–8 weeks, body weight of 20 ± 0.2 g) were purchased from Zhejiang Academy of Medical Sciences. Cytokine as well as Ig detecting ELISA kits were purchased from Langdun Biochemical Technology (Shanghai, China). The assay kits for T-AOC, SOD, GSH-Px, CAT and MDA were obtained from solarbio Biochemical Technology (Shanghai, China). Trifluoroacetate (TFA), 1-phenyl-3-methyl-5-pyrazolone (PMP), sugar standards and other chemical reagents were purchased from Aladdin Biochemical Technology (Shanghai, China).

2.2. Isolation and purification of the polysaccharide

The plant material of *U. longissima* was air dried and then powdered using a grinder. The dry powder was soaked in acetone and extracted for 12 h in a Soxhlet extractor. The crude polysaccharide from the solution was extracted using 1% cellulase (*w*/*v*) at 50 °C for 4 h, and the temperature was raised to 80 °C for 4 h. The supernatant of the extract was concentrated to one-tenth the original volume.

* Corresponding authors.
E-mail addresses: cyancy@zjou.edu.cn (Y. Chen), mojojo1984@163.com (Y. Chen).

https://doi.org/10.1016/j.ijbiomac.2021.03.183
0141-8130/

Four volumes of 95% ethanol were added to precipitate the polysaccharide. The precipitate was redissolved in water after centrifugation (1800 ×*g*, 10 min) and dialyzed against running water for 48 h (MwCO of dialysis bag, 3500). Lastly, the solution was lyophilized to acquire the crude polysaccharide [8].

The crude polysaccharide dissolved in distilled water (5 mg/mL) was centrifuged to obtain the supernatant, which was loaded onto an anion-exchange Q Sepharose Fast Flow column (300 × 30 mm) (GE Healthcare Co., Sweden). The sample in the column was eluted sequentially using distilled water and NaCl solutions with different concentrations (0.1–2 M). The fractions with high polysaccharide content were monitored spectrophotometrically using the phenol-sulfuric acid method [9]. The polysaccharide-containing fractions were collected, dialyzed, and lyophilized as described earlier. The main fraction eluted with 0.1 mol/L NaCl solution was collected and named CSL-0.1 [10].

2.3. Monosaccharide composition

The polysaccharide was dissolved in 2 M trifluoroacetate (TFA), completely hydrolyzed at 120 °C for 2 h, then the TFA were evicted by ethanol through rotary evaporation. Monosaccharide composition was measured by high performance liquid chromatography (HPLC) and UV detector (Agilent Technologies with 1200 Series detector) [11] after pre-column derivatization with 1-phenyl-3-methyl-5-pyrazolone (PMP). The standards are composed of L-arabinose (Ara), L-fucose (Fuc), D-galactose (Gal), D-galacturonic acid (GalUA), D-glucose (Glc), *N*-acetyl-β-D-glucosamine (GlcNAc), D-glucuronic acid (GlcUA), D-mannose (Man), L-rhamnose (Rha) and D-xylose (Xyl). Monosaccharide composition was identified by comparing the peak time between CSL-0.1 and standard sugars.

2.4. General properties and determination of the molecular weight

Total sugar content of CSL-0.1 was measured by the phenol-sulfuric acid method using glucose as a standard. Protein content was measured by the method of Bradford [12]. Uronic acid content was measured by the method of carbazole [13]. Molecular weight of CSL-0.1 was analyzed by high performance gel permeation chromatography (HPGPC) coupled with a TSKgel G3000PWXL column (7.8 mm × 30.0 cm, Tosoh, Japan) with refractive index detector. The CSL-0.1 was applied to the column at 35 °C and eluted with 0.2 mol/L Na_2SO_4 at a flow rate of 0.5 mL/min. A series of dextran standards (Mw: 70.8, 34.4, 20.0, 10.7, 4.71, 2.11, 9.6 and 5.9 kD) were performed as column calibration. Then the molecular weight of CSL-0.1 was estimated by GPC software [14].

2.5. IR spectroscopy

The sample of CSL-0.1 was ground with dried KBr powder and then pressed into a 1 mm transparent pellet. The CSL-0.1 pellet was measured for FTIR on Nicolet Omnic software and the Nicolet Nexus 470 instrument in the frequency range of 4000–500 cm^{-1} at the resolution of 4.0 cm^{-1} with background scanning frequency of 32 [15].

2.6. Gradual acid hydrolysis

The polysaccharide sample was hydrolyzed using 0.05 mol/L TFA at 100 °C for 2 h and then the hydrolysate was concentrated and evaporated with methanol to remove the TFA. Next, four volumes of ethanol were added to the hydrolysate and stored at 4 °C overnight. The supernatant, S-1, and the precipitate, P-1, were separated after centrifugation. P-1 was further hydrolyzed using 0.1 mol/L TFA for 1 h at 100 °C. After the removal of TFA and the addition of ethanol as described earlier, the supernatant that was obtained was named S-2 and the precipitate, P-2. S-1, S-2, and P-2 were completely hydrolyzed using 2 mol/L TFA for 3 h at 120 °C and the monosaccharide composition was determined [6].

2.7. Methylation analysis

The CSL-0.1 and the product after gradual acid hydrolysis P-2 were methylated by the method of modified Hakomor using NaH in DMSO and CH_3I. Then the methylated sample was hydrolyzed as above to cut the linkage of polysaccharide. The products were converted into partially methylated alditol acetates after reduced with $NaBH_4$ sodium. The alditol acetates sample was analyzed by GC–MS on a HP6890II/5973 instrument using a DB-5 ms fused silica capillary column (0.25 mm × 30 m) (Agilent Technologies Co., Ltd., USA) [16].

2.8. NMR spectroscopy

100 mg CSL-0.1 was dissolved in 1 mL D_2O, the sample solution was freeze dried for three times to completely replace H_2O with D_2O. The replaced sample was dissolved in D_2O at room temperature and analyzed using an Agilent DD2-600 MHz nuclear magnetic resonance spectrometer (Agilent Technologies) [15].

2.9. Evaluation of the immunostimulating and antioxidant effects of CSL-0.1

2.9.1. Animal experiments

Female ICR mice (6–8-week-old, body weight 20 ± 0.2 g) were purchased from the Zhejiang Academy of Medical Sciences. The mice were allowed to acclimatize to an SPF environment. They were housed at a room temperature of 23 ± 2 °C and a relative humidity of 50 ± 5%, and subjected to a 12:12-h light:dark cycle for one week before experiments. All animal experiments adhered to the strict guidelines of the Animal Ethics Committee of the School of Medicine and Pharmacy, Zhejiang Ocean University, regarding the humane use and care of animals.

For in vivo studies, mice were randomly divided into six groups (six mice for every group). The animals in the normal control group (NC) were administered physiological saline (0.9%) once daily for 10 days. The remaining mice received an intraperitoneal injection of 80 mg/kg cyclophosphamide (CP), once daily, for three consecutive days. The animals in the model control group (MC) received an intragastric injection of physiological saline for seven days and comprised mice that received the intraperitoneal CP injection. The animals in the positive control group (PC) were selected from the CP-injected mice, and received an intragastric injection of 40 mg/kg levamisole for seven days. The mice in the CSL-L, CSL-M, and CSL-H groups received an intragastric injection of 50 mg/kg, 100 mg/kg, and 200 mg/kg CSL-0.1, respectively for seven days. Similar to the other groups, these three groups comprised mice that had received the intraperitoneal injection of CP.

Animals in each group were sacrificed using an ethical procedure after fasting for 24 h. Blood from the mice eyeballs was collected and the serum was separated by centrifugation. The small intestine, spleen, thymus, and liver were collected, weighed, and stored at −80 °C until subsequent experiments [17].

2.9.2. Measurement of the spleen and thymus indices

The mice were weighed daily during the experiment. The spleens and thymi of mice were collected and weighed after the mice were sacrificed using cervical dislocation. The spleen and thymus indices were measured using the following equation [18]:

$$\text{spleen/thymus index} = \text{the weight of spleen/thymus (mg)}/[\text{the weight of mice (g)}*10]$$

2.9.3. Detection of secretory immunoglobulins A (Sig A) and serum cytokines

The intestinal fluid of experimental mice was collected and purified using cryogenic centrifugation. Sig A levels were measured using the supernatant of intestinal fluid by using an ELISA assay kit according to the

manufacturer's instructions. Blood samples were acquired by the enucleation of the mice eyeballs. Next, the serum was collected from the supernatant by centrifuging the blood samples at 1006 ×*g* for 10 min. Serum cytokine levels (IL-2, IL-4, IL-10, IFN-γ, and TNF-α) were measured using ELISA kits.

2.9.4. Determination of T-AOC, SOD, GSH-Px, CAT, and MDA levels

The intestinal fluid and liver homogenate were collected and the samples were purified using centrifugation at 1006 ×*g* for 10 min. The supernatants were used to determine the levels of T-AOC, SOD, GSH-Px, CAT, and MDA using assay kits per manufacturer's instructions.

2.9.5. Statistical analysis

Data obtained in this study were processed statistically and divergences are presented as mean ± SD. SPSS 16.0 for Windows was used and $P < 0.05$ indicated differences that were statistically significant.

3. Results and discussion

3.1. Extraction, purification, and characterization of the polysaccharide

The yield of the crude polysaccharide from *U. longissima* extracted using hot water and enzyme treatment was 7%. The crude polysaccharide was purified using Q Sepharose Fast Flow column to obtain the CSL-0.1 fraction after eluting with 0.1 M NaCl (Fig. 1a) and the yield was 28.9%. The molecular weight of CSL-0.1 was determined using high-performance gel permeation chromatography (HPGPC) (Fig. 1b). A single symmetrical peak obtained using HPGPC indicated that the polysaccharide was adequately pure to be used for structure elucidation. Based on the calibration curve constructed using standard dextran solutions, the molecular weight of CSL-0.1 was determined to be 7.86 × 10^4 Da.

The monosaccharide composition of CSL-0.1 was identified by matching the relative retention time (Fig. 1c) with their respective standards. It can be seen in Fig. 1d that CSL-0.1 is composed of mannose (Man), rhamnose (Rha), glucose (Glc), and galactose (Gal) in a ratio of 3.5:0.35:3.1:5 ratio. The total carbohydrate content was determined to be 80%, whereas the protein content was 6.7%. No uronic acid was detected. These findings corresponded with the monosaccharide composition of CSL-0.1.

3.2. IR spectroscopy

The FT-IR spectrum of CSL-0.1 is shown in Fig. 2. The absorption band at 3413 cm^{-1} is characteristic of —OH. The absorption peaks at 2930 cm^{-1} are associated with the C—H antisymmetric stretching vibration. The signal peak at 1642 cm^{-1} is attributed to the O—H stretching vibration. The absorption peaks at 1417 cm^{-1} and 1387 cm^{-1} can be ascribed to the C—H bending vibration. The two absorption bands at 1077 cm^{-1} and 1040 cm^{-1} are assigned to the stretching vibration of the C—O—C linkages indicating the characteristic feature of carbohydrates. The absorption band at 814 cm^{-1} is suggestive of the presence of mannose [19].

3.3. Partial acid hydrolysis

CSL-0.1 was found to be composed of Man, Rha, Glc, and Gal based on the monosaccharide composition. However, the monosaccharide distribution of CSL-0.1 was uncertain and variable. CSL-0.1 was gradually hydrolyzed using TFA to characterize the distribution of the monosaccharides in the molecule. In general, the side chains are easier to

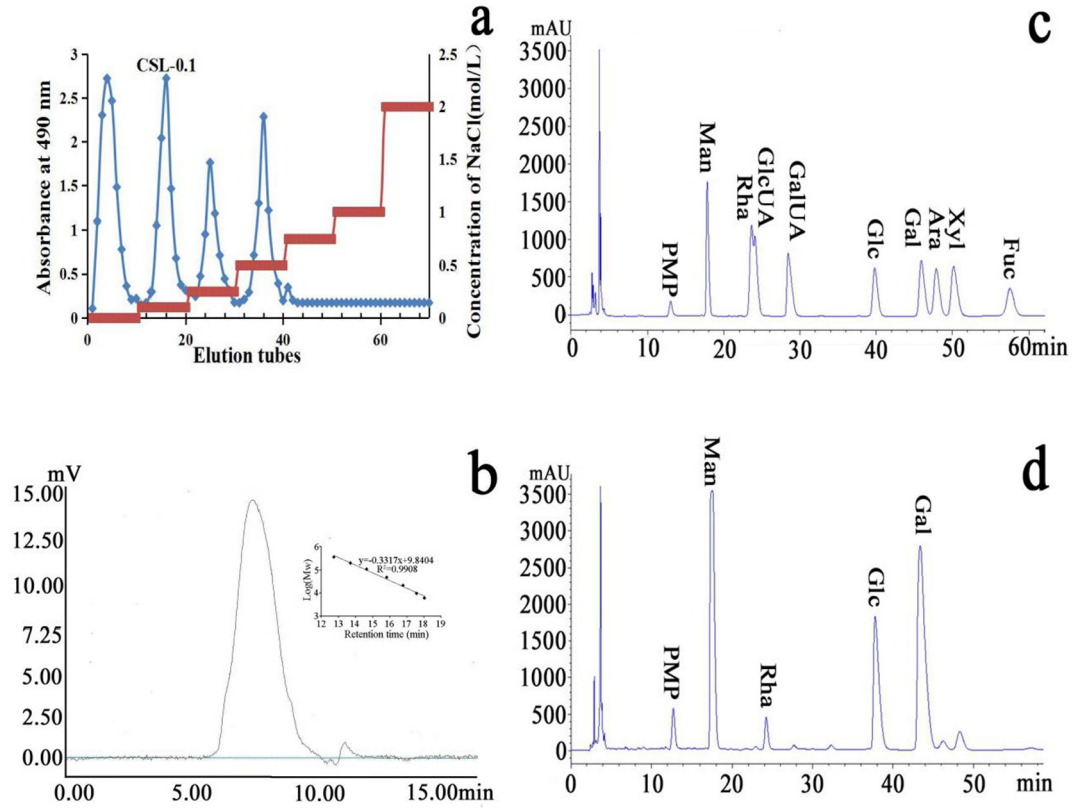

Fig. 1. Isolation, purification, HPGPC, and monosaccharide composition of CSL-0.1 extracted from *Usnea longissima*. (a) CSL-0.1 was obtained using Q Sepharose Fast Flow column after elution with 0.1 mol/L NaCl. (b) HPGPC chromatograms of CSL-0.1 on TSKgel G3000PWXL column and the standard curve of molecular weights. (c) HPLC chromatogram of standard monosaccharide mix. (d) HPLC chromatogram indicating the monosaccharide composition of CSL-0.1.

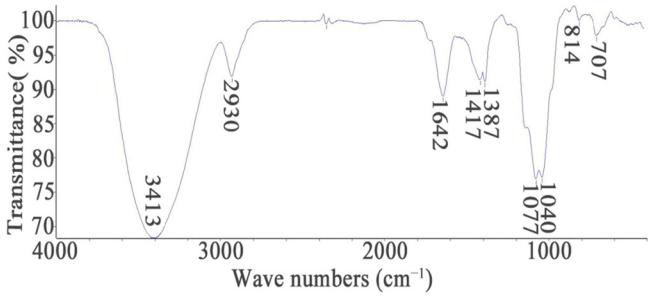

Fig. 2. IR spectroscopy of CSL-0.1.

hydrolyze than the mother chain. The structure of the backbone and side chains can be elucidated by analyzing the monosaccharide composition of CSL-0.1 after gradual hydrolysis [20].

The three fractions that were obtained after gradual acid hydrolysis were named S-1, S-2, and P-2. The monosaccharide composition of these three products is shown in Table 1. S-1 was found to be mainly composed of Glc and Gal, indicating that Glc and Gal were the major constituents of peripheral chains and are sensitive to acid hydrolysis. After the second hydrolysis with an increased acid concentration, the Glc and Gal content decreased, while that of Man and Rha increased, indicating the monosaccharide composition of S-2. In P-2, the amounts of Glc and Gal was reduced to 22.9% and 11.6%, respectively. Both Man and Rha content increased rapidly. Man was the major constituent of P-2 and accounted for 53.3% of the total sugars, indicating that it was mainly distributed in the mother chain. Rha was also located in the backbone to a lesser extent, whereas Glc and Gal were mainly present in the side chains [21].

3.4. Methylation analysis

CSL-0.1 and P-2 were permethylated, hydrolyzed, reduced, and finally acetylated for GC–MS to determine the linkage information of the polysaccharides. The linkage patterns of CSL-0.1 and its core structure P-2 are shown in Table 2. CSL-0.1 predominantly contained ten different glycosidic linkages; the Gal part of CSL-0.1 contained terminal Gal*f*, 1,6-linked Gal*f*, the MS spectrum of which were typical and very different from any of Gal*p* linkages; the linkages of Glc included 1,3-linked Glc*p* and 1,4-linked Glc*p*; the Man in CSL-0.1 was composed of 1,2-linked Man*p*, 1,6-linked Man*p*, 1,2,6-linked Man*p*, and 1,3,6-linked Man*p*. All the Rha sugars in CSL-0.1 had 1,2,3-linked Rha*p* linkages. 1,2-linked Rha*p*, 1,6-linked Man*p*, and 1,2,6-linked Man*p* constituted the primary composition of P-2, compared to Gal and Glc. The ratio of 1,2-linked Rha*p*, 1,6-linked Man*p*, and 1,2,6-linked Man*p* in P-2 was higher than that in CSL-0.1, which proves that 1,2,3-linked Rha*p*, 1,6-linked Man*p*, and 1,2,6-linked Man*p* were the primary linkages in the CSL-0.1 backbone. The increased distribution of 1,2-linked Rha*p* in P-2 indicated that side chains of CSL-0.1 were linked to the *O*-3 position of Rha. The distribution of the glycosidic bond patterns in the side chains consisted of terminal β-Gal*f*, 1,6-linked Gal*f*, 1,3-linked Glc*p*, and 1,4-linked Glc*p*.

Table 1
Monosaccharide composition of CSL-0.1, S-1, S-2, and P-2.

Sample	Monosaccharide composition (% m/m)			
	Man	Rha	Glc	Gal
CSL-0.1	29.3	2.9	25.9	41.9
S-1	7.8	0.9	52.6	38.7
S-2	34.3	9.5	42.2	14
P-2	53.3	12.2	22.9	11.6

3.5. NMR spectroscopy

NMR was used to characterize CSL-0.1. In ^{1}H NMR (Fig. 3a) combined with 2D-NMR (COSY, HSQC, HMBC, NOESY, and TOCSY spectra), a peak at 5.27 ppm was observed as two overlapped anomeric protons, which are labeled **A$_1$** and **A$_2$**. In addition, seven dominant anomeric proton signals were observed at 5.21, 5.07, 5.05, 5.00, 4.89, 4.82, and 4.28 ppm, which were designated as residues **B**, **C**, **D**, **E**, **F**, **G**, and **H**, respectively. In the ^{13}C NMR spectrum (Fig. 3b), the anomeric carbons at 99.9, 101.33, 99.47, 98.1, 107.1, 101.35, 107.99, 100.2, and 103.16 ppm were attributed to the residues **A$_1$**, **A$_2$**, **B**, **C**, **D**, **E**, **F**, **G**, and **H**, respectively, based on the direct connection of carbons to protons in the HSQC spectrum (Fig. 3e) [22]. The signals at 107.1 and 107.99 ppm were attributed to the anomeric carbons of the β-galactofuranose units based on their extraordinary low-field resonances.

For residue **A$_1$**, the anomeric proton signal and its correlating anomeric carbon signal appeared at δ 5.27/99.9. The signals of the other protons, H2, H3, H4, and H5, were identified as 3.55, 4.0, 3.69, and 3.98 ppm, respectively, based on the COSY (Fig. 3c) and TOCSY spectra (Fig. 3d). The corresponding carbons peaks at 71.7, 79.77, 71, and 73.2 ppm were assigned to C2, C3, C4, and C5, respectively [23], based on the C—H coupling seen in the HSQC spectrum. In general, most of the α-anomeric signals occur in the 5–6 ppm range while the β-anomeric proton was at 4–5 ppm regions [24]. Based on the results from the methylation analysis and reported literature, the downfield shift of C3 at 79.77 ppm suggested that residue **A$_1$** was a (1 → 3)-α-D-Glc*p* [25]. Similarly, the residues **A$_2$-H** were determined to be (1 → 2,3)-α-L-Rha*p* [26], (1 → 4)-α-D-Glc*p* [27], (1 → 2,6)-α-D-Man*p*, terminal β-D-Gal*f* [26], (1 → 2)-α-D-Man*p*, (1 → 6)-α-D-Gal*f*, (1 → 6)-α-D-Man*p* [28] and (1 → 4)-β-D-Glc*p* [23], respectively. Based on these results, the assignment of residues is summarized in Table 3.

The sequence of the linkage of the glycosidic residues was further deduced based on the HMBC (Fig. 3f) and NOESY spectra (Fig. 3g). In the HMBC spectrum, the H1 of residue **C** was related to C6 of residue **G**, which indicated that the (1 → 2,6)-α-D-Man*p* residue was linked to the *O*-6 position of (1 → 6)-α-D-Man*p*. The NOESY spectrum indicated that the H1 of residue **E** was related to H2 of residue **C** suggesting that (1 → 2)-α-D-Man*p* was connected to the *O*-2 position of (1 → 2,6)-α-D-Man*p*. These findings suggested that the Man of the polysaccharide could have a backbone consisting of (1 → 6)-α-D-Man*p*, in which the branch points were at the *O*-2 position and substituted by (1 → 2)-α-D-Man*p* as the side chains [29]. The HMBC spectrum revealed that the H1 of residue **A$_1$** was correlated with C4 of residue **B**, suggesting that the residue (1 → 3)-α-D-Glc*p* was linked to the *O*-4 of residue (1 → 4)-α-D-Glc*p*, and the existence of the faction, [3)-α-Glc*p*(1 → 4)-α-Glc*p*(1→]. Based on the NOESY spectrum, it was deduced that H1 of residues **D** and **F** corresponded to H4 of residue **B**, suggesting that the terminal β-D-Gal*f*(1 → and (1 → 6)-α-D-Gal*f* were also linked to the *O*-4 of residue (1 → 4)-α-D-Glc*p*. Furthermore, based on the NOESY spectrum, residue **F** correlated with the H3 of residue **A$_2$**, suggesting that (1 → 6)-α-D-Gal*f* was linked at the *O*-3 of residue (1 → 2,3)-α-L-Rha*p*. These findings, along with the results from the partial acid hydrolysis and methylation analysis, revealed that CSL-0.1 is likely a branched neutral heteropolysaccharide. It has a core structure with a (1 → 6)-α-D-Man*p* backbone and 60% of the residues in the backbone branched mainly at the *O*-2 position. (1 → 2)-α-L-Rha*p* could also be located in the backbone. The side chains were composed of (1 → 2)-α-D-Man*p* and (1 → 4)-α-D-Glc*p*. (1 → 3)-α-D-Glc*p* and terminal β-D-Gal*f*(1 → and (1 → 6)-α-D-Gal*f*, which were located at the end of the Man core were mostly linked to (1 → 4)-α-D-Glc*p*. Some of the (1 → 6)-α-D-Gal*f* residues could be linked to the *O*-3 of residue (1 → 2)-α-L-Rha*p*. Based on these analyses, a likely primary structure for CSL-0.1 was proposed (Fig. 4).

Lichens have been used as medicine and animal food for decades and their polysaccharide content is correlated to their beneficial effects to

Table 2
GC–MS analysis of CSL-0.1 and P-2.

Methylation product	Linkage type	Main MS (*m*/*z*)	Molar ratio (100%)	
			CSL-0.1	P-2
1,2,5-Ac_3-3,4-Me_3-D-Rha	→2)Rha*p*(1→	131, 189	–	12.1
1,2,3,5-Ac_4-4-Me_2-D-Rha	→2,3)Rha*p*(1→	127, 131, 261	3	–
1,3,5-Ac_3-2,4,6-Me_3-D-Glc	→3)Glc*p*(1→	101, 117, 129, 161, 233	15.6	7.4
1,4,6-Ac_2-2,3,5-Me_4-D-Gal	→6)Gal*f*(1→	101,117, 127, 233	1.4	–
1,4-Ac_2-2,3,5,6-Me_4-D-Gal	Gal*f*(1→	101, 117, 161, 205, 277	40.1	6.6
1,4,5-Ac_3-2,3,6-Me_3-D-Glc	→4)Glc*p*(1→	101, 113, 117, 131, 161, 173, 233	10.5	22
1,2,5-Ac_3-3,4,6-Me_3-D-Man	→2)Man*p*(1→	129, 161, 189	4.4	–
1,5,6-Ac_3-2,3,4-Me_3-D-Man	→6)Man*p*(1→	101, 117, 129, 161, 189	10.5	26.9
1,3,5,6-Ac_4-2,4-Me_2-D-Man	→3,6)Man*p*(1→	117, 129, 189, 233	1.9	–
1,2,5,6-Ac_4-3,4-Me_2-D-Man	→2,6)Man*p*(1→	129, 189	12.6	25

some extent. Among the identified lichens, the polysaccharides and chemicals constituents of about 100 species have been studied [30]. Three classes of polysaccharides are found in lichens, namely, β-glucans, α-glucans (linear or lightly substituted), and galactomannans (branched). The galactoglucomannans isolated from the mycobiont of *Parmotrema* species comprise (1 → 6)-α-D-Man*p* units as the main chain, which are preferentially substituted at the *O*-2 by the side chains containing a nonreducing end, 2-*O*- and 6-*O*-substituted α-Man*p* units. The galactomannan fractions from the lichen, *Roccella decipiens*, have a similar α-D-Man*p* core structure, but with side chains containing terminal-, 5-*O*-, 6-*O*-, and 5,6-di-*O*-substituted β-D-Gal*f* units. The heteropolysaccharide, xylorhamnogalactofuranan, isolated from *Cladina confuse* consists of (1 → 3)-linked galactofuranosyl units with side chains of 5-*O*- and 6-*O*-substituted Gal*f* units, as well 2-*O*-, 3-*O*-, and 2,3-di-*O*-substituted Rha*p*. A glucan with α-(1 → 3) (1 → 4) linkage has also been found in *Evernia prunastri* [31]. CSL-0.1 that was isolated in our study was found to have the combined characteristics of the polysaccharides described above. First, it shows a core mannan structure with (1 → 6)-linked α-Man*p* units as the main chain as the mycobiont of *Parmotrema* species. It shows the presence of terminal and 6-*O*-substituted β-D-Gal*f* units in the side chain, which is similar to the galactomannan present in *Roccella decipiens*. 2-*O*- and 2,3-di-*O*-substituted Rha*p* have also been reported to be present in the xylorhamnogalactofuranan of *Cladina confuse*. Although CSL-0.1 has no α-(1 → 3) (1 → 4) linked glucan in the main chain, it shows the presence of this component in the side chain. Thus, we can infer that the polysaccharide in *U. longissima* is a typical lichen polysaccharide.

3.6. Immunostimulating effects of CSL-0.1

Many lichens are known to have immunostimulating, antitumor, and antioxidant properties, which can mostly be attributed to the polysaccharides [32]. A study on the immunostimulating activities of an aqueous extract of *Cetraria islandica* indicates its ability to upregulate IL-10 secretion. Interestingly, only the polysaccharides among the secondary metabolites in the extract had anti-inflammatory effects [33]. It has been reported that a β-galactofuranose-containing polysaccharide isolated from the lichen, *Ramalina gracilis*, has in vitro cell eliciting activity on peritoneal macrophage [30]. A study on four lichen polysaccharides (three heteroglycans and a galactofuranorhamnan) from *Thamnolia* showed an immunostimulating effect on the human immune system [34]. In particular, the unusual galactofuranorhamnan was likely responsible for the immunostimulating activity.

As a medicinal lichen, *U. longissima* has been reported to have immunostimulating activity; however, the specific component responsible for activity has not been reported. Therefore, we conducted an in vivo study using a mouse model to determine if CSL-0.1 isolated from our study had immunostimulating effects.

3.6.1. Effect of CSL-0.1 on the spleen and thymus indices

Spleen and thymus are important immune organs. Their volume and weight decrease with a decline in immune function; therefore, these organ indices can reflect immune function and prognoses. An obvious decrease in the spleen and thymus indices were observed in the model group compared to that in the normal control group, indicating that CP weakened the immune system in mice (Fig. 5). Treatment with CSL-0.1 increased the spleen and thymus indices in a dose-dependent manner, relative to the MC group ($p < 0.05$), indicating that CSL-0.1 could alleviate the CP-induced shrinkage of immune organs. Especially for the high dose group with CSL-0.1 (CSL-H), the spleen and thymus indices increased by 35% and 50% compared to the MC group.

3.6.2. Effect of CSL-0.1 on cytokine and Sig A levels

Cytokines are low-molecular-proteins secreted by the monocyte-macrophages and lymphocytes and can regulate the immune system. IL-2, IL-4, IL-10, IFN-γ, TNF-α are important cytokines that play a crucial role in immunoregulation. In this study, we determined the changes in IL-2, IL-4, IL-10, IFN-γ, TNF-α levels in mice (Fig. 6a–e). Our findings showed that the expression of these cytokines was significantly reduced by CP; however, the changes were considerably reversed after CSL-0.1 treatment and levamisole administration. These results indicated that CP treatment for three consecutive days destroyed the immune balance. Treatment with CSL-0.1 increased the expression of IL-2, IL-4, IL-10, and IFN-γ in a dose-dependent manner (increased by 20%–30% compared to the MC group). For the cytokine TNF-α, mice treated with CSL-0.1 showed an increase in TNF-α level compared to those in the CP group. However, a decreasing trend was observed in the expression of TNF-α with increasing CSL-0.1 concentrations. It meant CSL-0.1 could remarkely increase the expression of TNF-α in a lower dose. Collectively, these results indicated that CSL-0.1 could promote the secretion of these cytokines, resulting in a reduction in the severity of immunosuppression [35].

The immune system functions based on complex cell-cell communication. T helper cells (Th1 and Th2) can lead to different functional properties because of different patterns of lymphokine secretion. Th1 promote the secretion of IL-2, TNF-α, and IFN-γ, whereas IL-4 and IL-10 release is governed by Th2; therefore, studying only the expression of single Th1 or Th2 cytokines may be insufficient. To further study immunoregulation based on the dynamic balance and mutual adjustment of Th1 and Th2, the following formula was selected as a reference of Th1/Th2 balance to analyze the immunoregulatory effect of CSL-0.1 [18].

$$\mathrm{Th1/Th2} = (\mathrm{IFN{-}\gamma + TNF{-}\alpha + IL{-}2})/(\mathrm{IL{-}4 + IL{-}10})$$

The Th1/Th2 ratio in the group with CP-injected mice was significantly increased compared to those in the NC group (Table 4). The Th1/Th2 ratio in the PC group was decreased to normal level. The

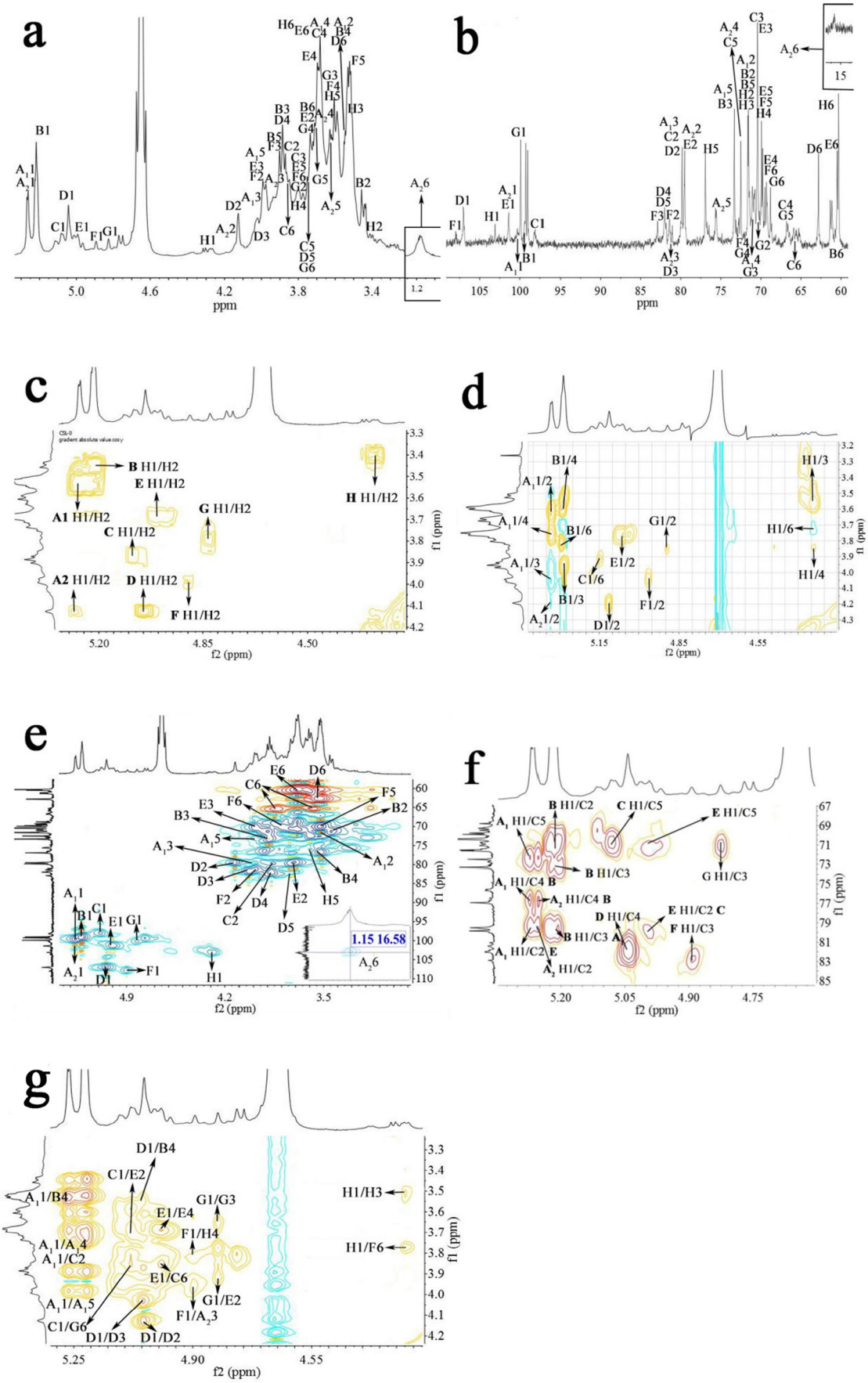

Fig. 3. NMR spectrum of CSL-0.1. (a) ^{1}H NMR spectrum; (b) ^{13}C NMR spectrum; (c) ^{1}H—^{1}H COSY spectrum in the anomeric region (residues **A$_1$-H**); (d) ^{1}H—^{1}H TOCSY spectrum of the anomeric residues; (e) HSQC spectrum of CSL-0.1; (f) ^{1}H—^{13}C HMBC spectrum in the anomeric region; (g) ^{1}H—^{1}H NOESY spectrum of the anomeric residues.

Table 3
^{1}H and ^{13}C NMR chemical shifts (δ) for the residues A_1-H of CSL-0.1.

Residue	H1/C1	H2/C2	H3/C3	H4/C4	H5/C5	H6/C6	Glycosidic correlation
A_1	5.27	3.55	4	3.69	3.98	–	C4 of **B**
→3)-α-D-Glc*p*(1→	99.9	71.7	79.77	71	73.2	–	
A_2	5.25	4.15	3.98	3.66	3.64	1.15	
→2,3)-α-L-Rha*p*(1→	101.33	79.38	81.32	72.45	74.55	16.6	
B	5.21	3.46	3.89	3.55	3.9	3.7	
→4)-α-D-Glc*p*(1→	99.47	71.57	73.35	76.84	71.48	60.9	
C	5.07	3.87	3.8	3.68	3.75	3.55, 3.84	C6 of **G**
→2,6)-α-D-Man*p*(1→	98.1	79.66	70.34	66.54	72.34	65.47	
D	5.05	4.14	4.05	3.88	3.76	3.54	H4 of **B**
β-D-Gal*f*(1→	107.1	80	81	82.12	82.29	62.84	
E	5	3.71	3.99	3.69	3.81	3.68	H2 of **C**
→2)-α-D-Man*p*(1→	101.35	79.55	70.26	69.11	70.02	60.69	
F	4.89	3.99	3.9	3.6	3.51	3.78	H4 of **B**
→6)-α-D-Gal*f*(1→	107.99	81.52	83	72	69.7	69	H3 of **A2**
G	4.82	3.8	3.66	3.74	3.71	3.75, 3.85	
→6)-α-D-Man*p*(1→	100.2	70.14	70.88	72.1	66.52	68.85	
H	4.28	3.4	3.5	3.8	3.61	3.68	
→4)-β-D-Glc*p*(1→	103.16	71.3	71.69	76	–	–	

CSL-treatment groups also showed the downregulation of Th1/Th2 in a dose-dependent manner. For CSL-H, it almostly had the same effect as PC group to decrease the Th1/Th2 ratio to normal level. Moreover, our results indicated that CSL-0.1 exerted its immunostimulating effects by reversing the Th1/Th2-related cytokine imbalance induced by CP treatment. CSL-0.1 effectively enhanced intestinal immunity and regulated the Th1/Th2 balance.

Sig A is the main antibody on the surface of human mucosa that plays a crucial role in intestinal immunity. Sig A levels were 30% lower in CP-treated mice compared to those in the NC group (Fig. 6f). This change was alleviated after levamisole administration, as observed in the PC group. A significant increase in Sig A level was observed in the CSL treatment groups in a dose-dependent manner (about 20% increase), indicating that CSL-0.1 could promote Sig A secretion and improve intestinal immunity [36].

3.6.3. Effect of CSL on antioxidant enzymes in the liver and intestine

Oxidative damage is caused by the excessive generation of free radicals and loss of antioxidant defense. SOD, GSH-Px, and CAT, as endogenous antioxidant enzymes, play a vital role in antioxidant defense. MDA is released during lipid peroxidation and is often used as an indicator of antioxidant activity [37].

To determine the effect of CSL-0.1 on the antioxidant enzymes, first, the activities of T-AOC, SOD, MDA, GSH-Px, and CAT in the liver and intestine were measured. CP injection in mice caused a remarkable decrease in the levels of T-AOC, SOD, GSH-Px, and CAT and an increase in MDA levels. After the mice were treated with CSL-0.1, the T-AOC, SOD, GSH-Px, and CAT levels in both the intestine (Fig. 7) and liver (Fig. 8) clearly increased by 20%–50%, while the level of MDA decreased to the same as the NC group at high dose group CSL-H.

It is widely known that the excessive reactive oxygen species (ROS) or reactive nitrogen species (RNS) induced oxidative stress will cause significant damage to cell structure and biomolecular function, directly or indirectly leading to a number of diseases [38]. 4-Hydroperoxy cyclophosphamide is the active metabolite form of the prodrug Cyclophosphamide. It crosslinks DNA and induces T cell apoptosis independent of death receptor activation, but activates mitochondrial death pathways through production of ROS, which has the potential for lymphomas and autoimmune disorders [39]. Accumulating evidence strongly suggests that oxidative stress is related to immune system dysfunction [40] and it is an important causative factor for immunodeficiency [41]. Polysaccharides are considered as effective free radical scavenger, reducing agent. They could reduce ROS directly or affect antioxidant enzymes. Thus, antioxidant polysaccharides are used to balance the oxidation condition of the body to reduce the toxicity of 4-Hydroperoxy cyclophosphamide. Immunostimulating polysaccharides play an important role in modulating the immune responses, of which the crosstalk between different immune cells results in the potentiation of cytokines and antibody production [42]. They can potentially modulate the host immune system to relieve the side reaction of Cyclophosphamide. Our results showed that CSL-0.1 possessed excellent antioxidant activities and immunostimulating effect, which could potentially be applied for the modulation of the host immune system. The internal relations between antioxidant activities and immunostimulating effect of CSL-0.1 may be partly due to the scavenging of the oxygen free radicals.

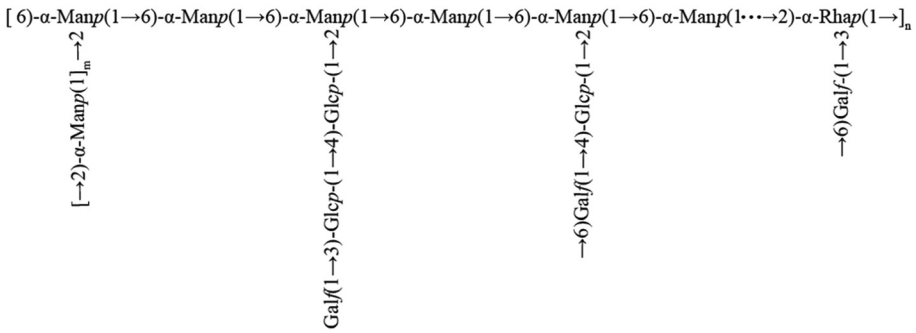

Fig. 4. Proposed structure of CSL-0.1.

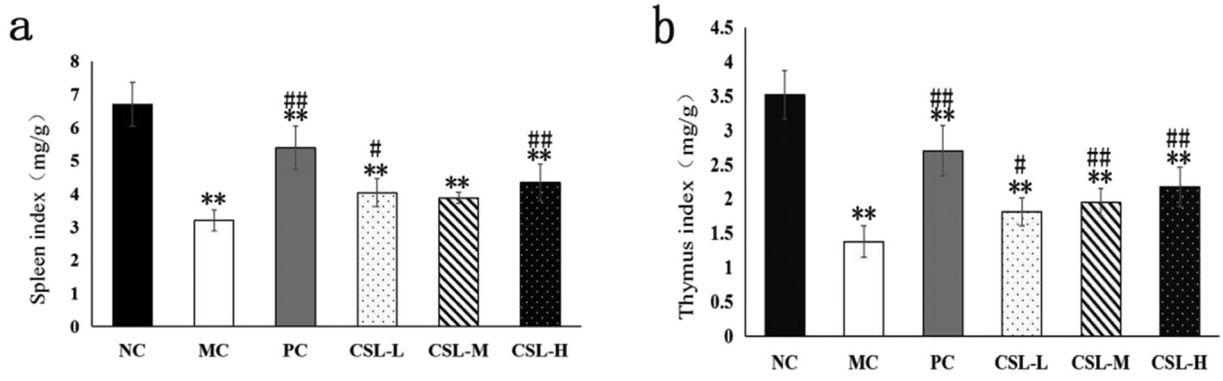

Fig. 5. Spleen and thymus indices after treatment with CP, levamisole, and CSL-0.1. (a) spleen index; (b) thymus index. The values are presented as mean ± SD, n-6. Significant differences with the NC group: $^{*}p < 0.05$ and $^{**}p < 0.01$; Significant differences with the MC group: $^{\#}p < 0.05$ and $^{\#\#}p < 0.01$.

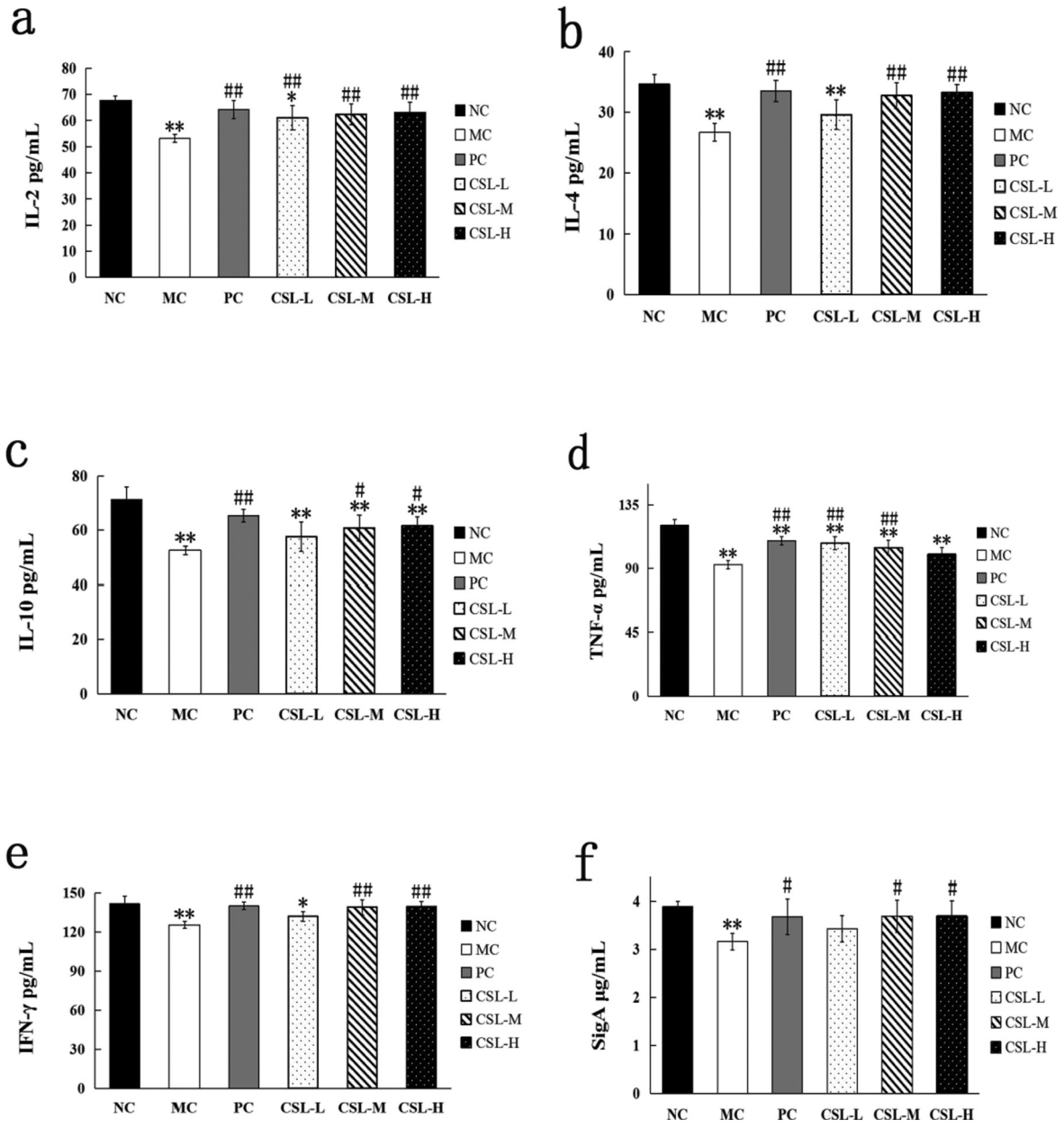

Fig. 6. Effect of CSL-0.1 on the secretion of immune factors in mice. (a) IL-2; (b) IL-4; (c) IL-10; (d) TNF-α; (e) IFN-γ; (f) Sig A. The values are presented as mean ± SD, n-6. Significant differences with the NC group: $^{*}p < 0.05$ and $^{**}p < 0.01$; Significant differences with the MC group: $^{\#}p < 0.05$ and $^{\#\#}p < 0.01$.

Table 4
Effect of CSL-0.1 on Th1/Th2 in CP-treated mice.

Treatment	NC	MC	PC	CSL-L	CSL-M	CSL-H
Th1/Th2	3.11 ± 0.13	3.42*±0.08	3.18# ± 0.14	3.41*±0.16	3.29# ± 0.25	3.19# ± 0.09

* $p < 0.05$ vs. control group.
\# $p < 0.05$ vs. model group.

4. Conclusions

In this study, we isolated a polysaccharide, CSL-0.1, from the lichen, *Usnea longissima*. CSL-0.1 was composed of Man, Rha, Glc, and Gal in the ratio of 3.5:0.35:3.1:5 and had a molecular weight of 7.86×10^4 Da. The polysaccharide had a core mannan structure with (1 → 6)-α-D-Man*p* units as the main chain and was substituted at the *O*-2 position with side chains containing (1 → 2)-α-D-Man*p* residue, the faction, [3)-α-Glc*p*(1 → 4)-α-Glc*p*(1→], a nonreducing end, and 6-*O*-substituted β-D-Gal*f* units. 2-*O*- and 2,3-di-*O*-substituted Rha*p* units were also found to be components of the polysaccharide.

Based on the spleen and thymus indices, we could infer that CSL-0.1 alleviates the CP-induced shrinkage of immune organs by enhancing the immune function of mice. In addition, CSL-0.1 could restore the balance of the immune system via regulating cytokine secretion. Besides, CSL-0.1 exerts antioxidant effects in the intestine and liver of immunosuppressed mice. To summarize, our study provides a basis and serves as a starting point for further research of *U. longissima*. The molecular mechanisms of immunostimulating activity and the detailed correlation between the structure and activities of polysaccharides from *U. longissima* need be determined in further study.

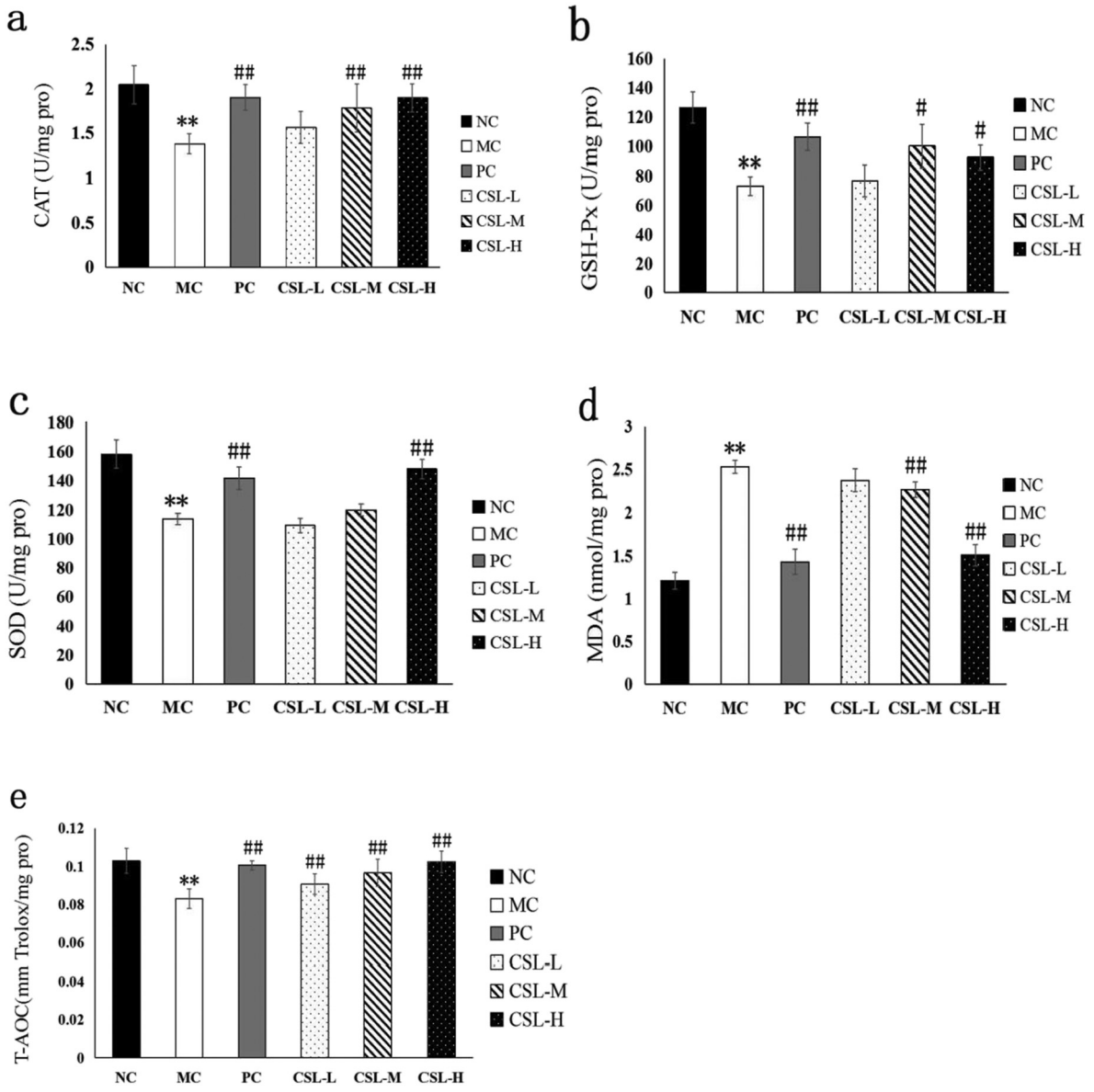

Fig. 7. Effects of CSL-0.1 on the antioxidant enzymes in the intestine of mice. (a) CAT; (b) GSH-Px; (c) SOD; (d) MDA; (e) T-AOC. The values are presented as mean ± SD, n-6. Significant differences with the NC group: *$p < 0.05$ and **$p < 0.01$; Significant differences with the MC group: #$p < 0.05$ and ##$p < 0.01$.

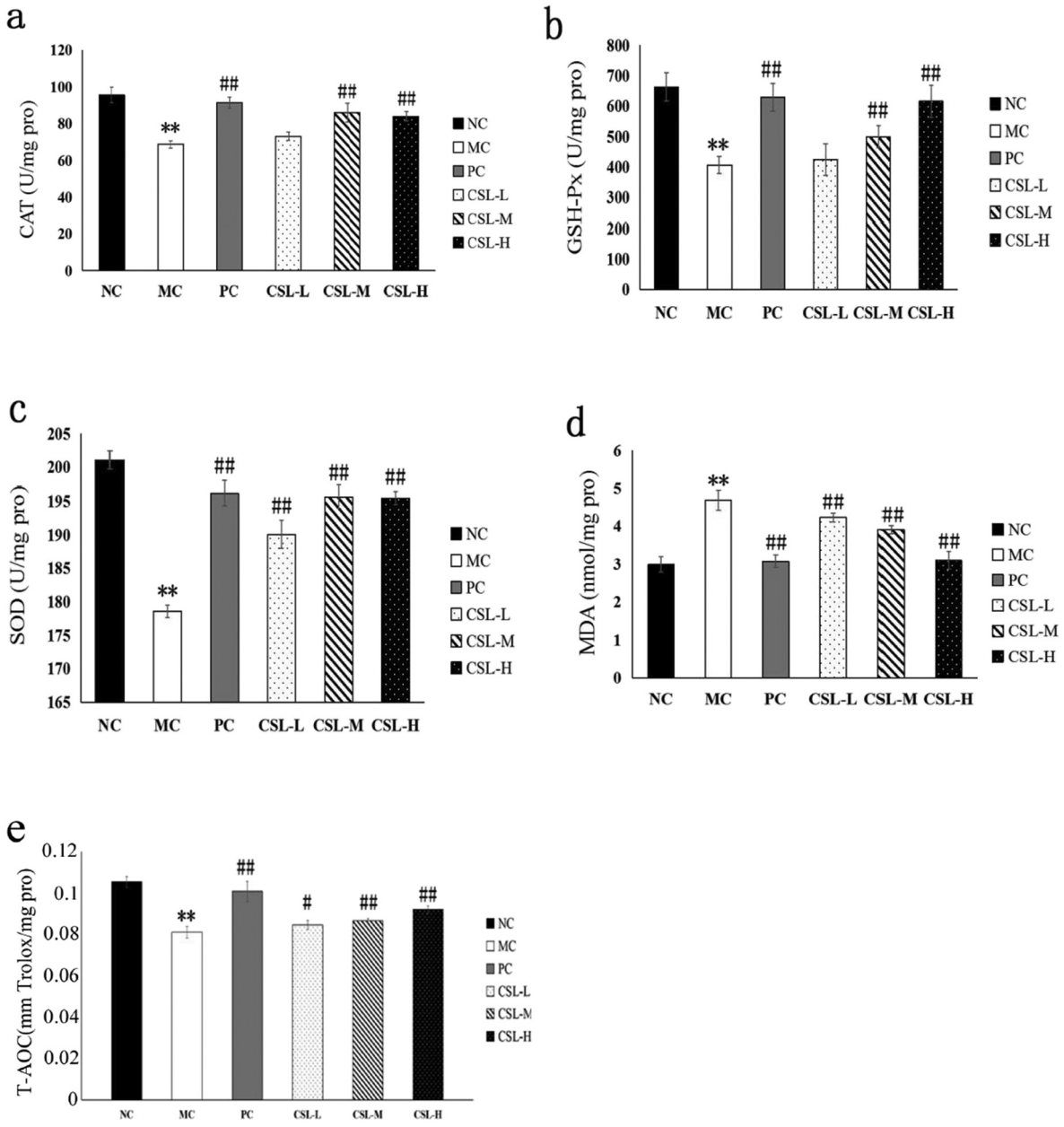

Fig. 8. Effects of CSL-0.1 on the antioxidant enzymes in the liver of mice. (a) CAT; (b) GSH-Px; (c) SOD; (d) MDA; (e) T-AOC. The values are presented as mean ± SD, n-6. Significant differences with the NC group: $^{*}p < 0.05$ and $^{**}p < 0.01$; Significant differences with the MC group: $^{\#}p < 0.05$ and $^{\#\#}p < 0.01$.

CRediT authorship contribution statement

Wang Teng: Writing - Original draft preparation. **Shen Chen**: Methodology on structure. **Guo Feng** and **Zhao Yuqin**: Methodology on bioactivity. **Wang Jie** and **Chen Yan**: Funding acquisition and review on NMR. **Sun Kunlai**: Sample preparation. **Chen Yin**: Funding acquisition, Writing - Reviewing and Editing. **Wang Bin**: Supervision and Conceptualization.

Declaration of competing interest

The authors declare that there are no conflicts of interest.

Acknowledgement

This work was supported by Natural Science Foundation of Zhejiang Province, China (LGF19D060004, LQ18D060005 and LGN18D060002); National Natural Science Foundation of China (41406142).

References

[1] Wang Yi, Juan Wang, Yong Hwa Cheong, Jae-Seoun Hur, Three new non-reducing polyketide synthase genes from the lichen-forming fungus *Usnea longissima*, Mycobiology (2014)https://doi.org/10.5941/MYCO.2014.42.1.34.

[2] M. Halici, F. Odabasoglu, H. Suleyman, A. Cakir, A. Aslan, Y. Bayir, Effects of water extract of *Usnea longissima* on antioxidant enzyme activity and mucosal damage caused by indomethacin in rats, Phytomedicine 12 (9) (2005) 656–662, https://doi.org/10.1016/j.phymed.2004.06.021.

[3] C.C. Grueter, D. Li, B. Ren, F. Wei, Z. Xiang, C.P.V. Schaik, Fallback foods of temperate-living primates: a case study on snub-nosed monkeys, Am. J. Phys. Anthropol. (2010) 700–715, https://doi.org/10.1002/ajpa.21024.

[4] K.A. Lee, M.S. Kim, Antiplatelet and antithrombotic activities of methanol extract of *Usnea longissima*, Phytother. Res. 19 (12) (2010) 1061–1064, https://doi.org/10.1002/ptr.1791.

[5] E. Yildirim, A. Aslan, B. Emsen, A. Cakir, S. Ercisli, Insecticidal effect of *Usnea longissima* (Parmeliaceae) extract against *Sitophilus granarius* (Coleoptera: Curculionidae), Int. J. Agric. Biol. (2012)https://doi.org/10.1071/AN11060.

[6] T. Wang, Z. Dong, D. Zhou, K. Sun, Y. Zhao, B. Wang, Y. Chen, Structure and immunostimulating activity of a galactofuranose-rich polysaccharide from the bamboo parasite medicinal fungus Shiraia bambusicola, J. Ethnopharmacol. 257 (2020), 112833, https://doi.org/10.1016/j.jep.2020.112833.

[7] X. Bian, J. Jin, D. Ding, H. Zhang, Study on the scavenging action of polysaccharide of *Usnea longissima* to oxygen radical and its anti-lipi peroxidation effects, Zhong Yao Cai 25 (3) (2002) 188–189, https://doi.org/10.1007/s007050050640.
[8] D. Zhou, P. Li, Z. Dong, T. Wang, K. Sun, Y. Zhao, B. Wang, Y. Chen, Structure and immunoregulatory activity of β-d-galactofuranose-containing polysaccharides from the medicinal fungus Shiraia bambusicola, Int. J. Biol. Macromol. 129 (2019) 530–537, https://doi.org/10.1016/j.ijbiomac.2019.01.179.
[9] T. Masuko, A. Minami, N. Iwasaki, T. Majima, S. Nishimura, Y.C. Lee, Carbohydrate analysis by a phenol–sulfuric acid method in microplate format, Anal. Biochem. 339 (1) (2005) 69–72, https://doi.org/10.1016/j.ab.2004.12.001.
[10] Y. Chen, W. Mao, Y. Yang, X. Teng, W. Zhu, X. Qi, Y. Chen, C. Zhao, Y. Hou, C. Wang, N. Li, Structure and antioxidant activity of an extracellular polysaccharide from coral-associated fungus, Aspergillus versicolor LCJ-5-4, Carbohydr. Polym. 87 (1) (2012) 218–226, https://doi.org/10.1016/j.carbpol.2011.07.042.
[11] J. Zhang, Q. Zhang, J. Wang, S.Z. Zhang, Analysis of the monosaccharide composition of fucoidan by precolumn derivation HPLC, Chin. J. Oceanol. Limnol. 27 (3) (2009) 578–582, https://doi.org/10.1007/s00343-009-9205-0.
[12] Marion M. Bradford, A rapid and sensitive method for the quantitation of microgram quantities of protein utilizing the principle of protein-dye binding, Anal. Biochem. 72 (1–2) (1976) 248–254, https://doi.org/10.1016/0003-2697(76)90527-3.
[13] Z. Dische, A modification of the carbazole reactin of hexuronic acid for the study of polyuronides, J. Biol. Chem. 183 (2) (1950) 489–494, https://doi.org/10.1515/bchm2.1950.285.4-5.238.
[14] Y. Chen, W.J. Mao, M.X. Yan, X. Liu, S.Y. Wang, Z. Xia, B. Xiao, S.J. Cao, B.Q. Yang, J. Li, Purification, chemical characterization, and bioactivity of an extracellular polysaccharide produced by the marine sponge endogenous fungus Alternaria sp. SP-32, Mar. Biotechnol. 18 (3) (2016) 301–313, https://doi.org/10.1007/s10126-016-9696-6.
[15] J.Y. Qian, W. Chen, W.M. Zhang, H. Zhang, Adulteration identification of some fungal polysaccharides with SEM, XRD, IR and optical rotation: a primary approach, Carbohydr. Polym. 78 (3) (2009) 620–625, https://doi.org/10.1016/j.carbpol.2009.05.025.
[16] X. Qi, W. Mao, Y. Gao, Y. Chen, Y. Chen, C. Zhao, N. Li, C. Wang, M. Yan, C. Lin, J. Shan, Chemical characteristic of an anticoagulant-active sulfated polysaccharide from *Enteromorpha clathrata*, Carbohydr. Polym. 90 (4) (2012) 1804–1810, https://doi.org/10.1016/j.carbpol.2012.07.077.
[17] S. Chen, J. Wang, Q. Fang, N. Dong, S. Nie, Polysaccharide from natural Cordyceps sinensis ameliorated intestinal injury and enhanced antioxidant activity in immunosuppressed mice, Food Hydrocoll. 89 (APR.) (2019) 661–667, https://doi.org/10.1016/j.foodhyd.2018.11.018.
[18] Y. Wang, Q. Qi, A. Li, M. Yang, W. Huang, H. Xu, Z. Zhao, S. Li, Immuno-enhancement effects of Yifei Tongluo Granules on cyclophosphamide-induced immunosuppression in Balb/c mice, J. Ethnopharmacol. 194 (2016) 72–82, https://doi.org/10.1016/j.jep.2016.08.046.
[19] Y. Bai, X. Jia, F. Huang, R. Zhang, L. Dong, L. Liu, M. Zhang, Structural elucidation, anti-inflammatory activity and intestinal barrier protection of longan pulp polysaccharide LPIIa, Carbohydr. Polym. 246 (2020), 116532, https://doi.org/10.1016/j.carbpol.2020.116532.
[20] X. Gao, H. Qu, S. Shan, C. Song, D. Baranenko, Y. Li, W. Lu, A novel polysaccharide isolated from *Ulva pertusa*: structure and physicochemical property, Carbohydr. Polym. 233 (2020), 115849, https://doi.org/10.1016/j.carbpol.2020.115849.
[21] L. Xia, M. Zhu Deji, D. Chen, Y. Lu, Juniperus pingii var. wilsonii acidic polysaccharide: extraction, characterization and anticomplement activity, Carbohydr. Polym. 231 (2020), 115728, https://doi.org/10.1016/j.carbpol.2019.115728.
[22] J. Chen, X. Zhang, D. Huo, C. Cao, Y. Li, Y. Liang, B. Li, L. Li, Preliminary characterization, antioxidant and α-glucosidase inhibitory activities of polysaccharides from Mallotus furetianus, Carbohydr. Polym. 215 (2019) 307–315, https://doi.org/10.1016/j.carbpol.2019.03.099.
[23] W.H.M.v. Casteren, C. Dijkema, H.A. Schols, G. Beldman, A.G.J. Voragen, Structural characterisation and enzymic modification of the exopolysaccharide produced by Lactococcus lactis subsp cremoris B39, Carbohydr. Res. 324 (3) (2000) 170–181, https://doi.org/10.1016/S0008-6215(00)00065-3.
[24] J. Gu, H. Zhang, J. Zhang, C. Wen, Y. Duan, Optimization, characterization, rheological study and immune activities of polysaccharide from *Sagittaria sagittifolia* L, Carbohydr. Polym. 246 (2020) 116595, https://doi.org/10.1016/j.carbpol.2020.116595.
[25] X. Zheng, H. Sun, L. Wu, X. Kong, Q. Song, Z. Zhu, Structural characterization and inhibition on α-glucosidase of the polysaccharides from fruiting bodies and mycelia of Pleurotus eryngii, Int. J. Biol. Macromol. 156 (2020) 1512–1519, https://doi.org/10.1016/j.ijbiomac.2019.11.199.
[26] I.A.I. Ali, Y. Akakabe, S. Moonmangmee, A. Deeraksa, M. Matsutani, T. Yakushi, M. Yamada, K. Matsushita, Structural characterization of pellicle polysaccharides of Acetobacter tropicalis SKU1100 wild type and mutant strains, Carbohydr. Polym. 86 (2) (2011) 1000–1006, https://doi.org/10.1016/j.carbpol.2011.05.055.
[27] Y. Liu, W. Liu, J. Li, S. Tang, M. Wang, W. Huang, W. Yao, X. Gao, A polysaccharide extracted from Astragalus membranaceus residue improves cognitive dysfunction by altering gut microbiota in diabetic mice, Carbohydr. Polym. 205 (2019) 500–512, https://doi.org/10.1016/j.carbpol.2018.10.041.
[28] Y. Li, L. You, F. Dong, W. Yao, J. Chen, Structural characterization, antiproliferative and immunoregulatory activities of a polysaccharide from Boletus Leccinum rugosiceps, Int. J. Biol. Macromol. 157 (2020) 106–118, https://doi.org/10.1016/j.ijbiomac.2020.03.250.
[29] Y. Chen, X. Ou, J. Yang, S. Bi, B. Peng, Y. Wen, L. Song, C. Li, R. Yu, J. Zhu, Structural characterization and biological activities of a novel polysaccharide containing N-acetylglucosamine from Ganoderma sinense, Int. J. Biol. Macromol. 158 (2020) 1204–1215, https://doi.org/10.1016/j.ijbiomac.2020.05.028.
[30] L. Cordeiro, S. Oliveira, D.F. Buchi, M. Iacomini, Galactofuranose-rich heteropolysaccharide from Trebouxia sp., photobiont of the lichen Ramalina gracilis and its effect on macrophage activation, Int. J. Biol. Macromol. 42 (5) (2008) 436–440, https://doi.org/10.1016/j.ijbiomac.2008.02.002.
[31] N. Karunaratne, U. Jayalal, V. Karunaratne, Lichen polysaccharides, The Complex World of Polysaccharides 2012, pp. 215–226 , Chapter.8 https://doi.org/10.5772/51021.
[32] E.S. Olafsdottir, K. Ingólfsdottir, Polysaccharides from lichens: structural characteristics and biological activity, Planta Med. 67 (3) (2001) 199–208, https://doi.org/10.1055/s-2001-12012.
[33] J. Freysdottir, S. Omarsdottir, K. Ingólfsdóttir, A. Vikingsson, E.S. Olafsdottir, In vitro and in vivo immunomodulating effects of traditionally prepared extract and purified compounds from *Cetraria islandica*, Int. Immunopharmacol. 8 (3) (2008) 423–430, https://doi.org/10.1016/j.intimp.2007.11.007.
[34] S. Omarsdottir, J. Freysdottir, E.S. Olafsdottir, Immunomodulating polysaccharides from the lichen *Thamnolia vermicularis* var. subuliformis, Phytomedicine 14 (2–3) (2007) 179–184, https://doi.org/10.1016/j.phymed.2006.11.012.
[35] S. Fan, S. Nie, X. Huang, S. Wang, J. Hu, J. Xie, Q. Nie, M. Xie, Protective properties of combined fungal polysaccharides from Cordyceps sinensis and Ganoderma atrum on colon immune dysfunction, Int. J. Biol. Macromol. 114 (2018) 1049–1055, https://doi.org/10.1016/j.ijbiomac.2018.04.004.
[36] X. Gao, J. Zhu, H. Luo, J. Yan, Y.M. Yao, Ovotransferrin enhances intestinal immune response in cyclophosphamide-induced immunosuppressed mice, Int. J. Biol. Macromol. (2018)https://doi.org/10.1016/j.ijbiomac.2018.08.058.
[37] H. Tian, H. Liu, W. Song, L. Zhu, T. Zhang, R. Li, X. Yin, Structure, antioxidant and immunostimulatory activities of the polysaccharides from *Sargassum carpophyllum*, Algal Res. 49 (2020), 101853, https://doi.org/10.1016/j.algal.2020.101853.
[38] J. Wang, S. Hu, S. Nie, Q. Yu, M. Xie, Reviews on mechanisms of in vitro antioxidant activity of polysaccharides, Oxidative Med. Cell. Longev. 2016 (64) (2015) 5692852, https://doi.org/10.1155/2016/5692852.
[39] R. Jeelani, S.N. Khan, F. Shaeib, H.R. Kohan-Ghadr, H.M. Abu-Soud, Cyclophosphamide and acrolein induced oxidative stress leading to deterioration of metaphase II mouse oocyte quality, Free Radic. Biol. Med. 110 (2017) 11–18, https://doi.org/10.1016/j.freeradbiomed.2017.05.006.
[40] R. Ahmad, C. Haldar, Immune responses to lipopolysaccharide challenge in a tropical rodent (Funambulus pennanti): photoperiod entrainment and sex differences, Stress Int. J. Biol. Stress 15 (2) (2012) 172–183, https://doi.org/10.3109/10253890.2011.606515.
[41] Y. Yan, L. Wanshun, H. Baoqin, W. Changhong, F. Chenwei, L. Bing, C. Liehuan, The antioxidative and immunostimulating properties of d-glucosamine, Int. Immunopharmacol. 7 (1) (2007) 29–35, https://doi.org/10.1016/j.intimp.2006.06.003.
[42] L. Ren, J. Zhang, T. Zhang, Immunomodulatory activities of polysaccharides from Ganoderma on immune effector cells, Food Chem. 340 (2021), 127933, https://doi.org/10.1016/j.foodchem.2020.127933.